

## Electronic Supplementary Information

### **Se-doped MoS<sub>2</sub> nanosheet for improved hydrogen evolution reaction**

Xianpei Ren,<sup>a</sup> Qiang Ma,<sup>a</sup> Haibo Fan,<sup>a, c</sup> Liuqing Pang,<sup>a</sup> Yunxia Zhang,<sup>a</sup> Yao Yao,<sup>a</sup>  
Xiaodong Ren,<sup>a</sup> Shengzhong (Frank) Liu<sup>a, b, \*</sup>

<sup>a</sup>Key Laboratory of Applied Surface and Colloid Chemistry, National Ministry of Education; Institute for Advanced Energy Materials, School of Materials Science and Engineering, Shaanxi Normal University, Xi'an 710119, China

<sup>b</sup>Dalian Institute of Chemical Physics, Dalian National Laboratory for Clean Energy, Chinese Academy of Sciences, Dalian, 116023, China

<sup>c</sup>School of Physics, Northwest University, Xi'an 710069, China

\*Corresponding author. E-mail: szliu@dicp.ac.cn; Tel: +86-29-8153-0785

## **Experimental Section**

### ***Reagents and materials***

Sodium molybdate, L-Ascorbic Acid and Diphenyl diselenide (DDS) were purchased from Aladdin Industrial Inc.  $\text{H}_2\text{SO}_4$  was purchased from Tianjin Fuyu Chemical Reagent Co. Ltd., China. Pt and glassy carbon electrodes were purchased from Tianjin Aidahengsheng Technology. Co. Ltd., China. All chemicals were used as received without further purification. The water used throughout all experiments was deionized (DI) water purified through a Millipore system.

### ***Preparation of Se-doped $\text{MoS}_2$ nanosheets***

The synthesis of Se-doped  $\text{MoS}_2$  nanosheets could be divided into 2 steps: (i) The mixture of 0.4 g of  $\text{Na}_2\text{MoO}_4 \cdot 2\text{H}_2\text{O}$  and 0.65 g of L-cysteine were dissolved in 60 mL DI water, and then transferred into a 100 mL Teflon-lined stainless steel autoclave and maintained at 180 °C for 18 hours. After cooling naturally to ambient temperature, the black precipitates were collected by centrifugation, washed with DI water and ethanol, dried in a vacuum oven at 80 °C for overnight and then the  $\text{MoS}_2$  powder was obtained. (ii) Se-doped  $\text{MoS}_2$  was synthesized by directly annealing  $\text{MoS}_2$  nanosheets and DDS in a conventional tube furnace in Ar/ $\text{H}_2$  atmosphere. As Se is insoluble in ethanol and water, it is difficult to distribute Se powder uniformly on the surface of the  $\text{MoS}_2$  nanosheets, we choose DDS as the Se dopant. The detailed procedure is as follows:  $\text{MoS}_2$  nanosheets (200mg) and DDS (78mg) were first ultrasonically dispersed in ethanol for about 30 min. The resulting suspension was spread onto an evaporating dish and dried, forming a uniform solid mixture. The mixtures were placed into a quartz tube with Ar/ $\text{H}_2$  atmosphere and annealed at 800°C for 2 hours. After that, the sample was cooled to room temperature under ambient Ar/ $\text{H}_2$  and collected from the quartz tube. For comparison, the  $\text{MoS}_2$  without any dopants was treated under the same condition.

### ***Characterization***

The Field emission transmission electron microscopy (FETEM) images were taken with a FEI Tecnai G2 F20. Field emission scanning electron microscope (FESEM) observations were performed on SU8020. X-ray photoelectron

spectroscopy (XPS) experiments were made on an AXISULTRA. Raman spectrum at excitation wavelength of 532 nm was obtained from a Renishaw Invia Raman microscope. X-ray diffraction (XRD) patterns were obtained on a DX-2700 diffractometer.

### ***Electrochemical characterization***

Electrochemical measurements were carried out with a computer-controlled IM6ex (Zahner, Germany) in a standard three-electrode cell using Ag/AgCl (in 3.5 M KCl solution) electrode as the reference electrode, a platinum foil as the counter electrode and the glassy carbon (GC) electrodes modified with catalyst as the working electrode. The working electrode was fabricated as follows: 4 mg of catalyst and 80  $\mu$ L of 5 wt% Nafion solution were dispersed in 1 mL of a solution of deionized water and ethanol (4:1 in volume ratio). After stirring by ultrasonication for 1 h, 5  $\mu$ L of the resulting solution was dropcast onto the top of a glassy carbon electrode with 3 mm diameter. The catalyst-coated GC electrode was dried at 80 °C for 2 h to yield a catalyst loading of 0.285 mg/cm<sup>2</sup>. Linear sweep voltammetry (LSV) with scan rate of 10 mV/s was conducted in 0.5 M H<sub>2</sub>SO<sub>4</sub> (purged with pure N<sub>2</sub>). The electrochemical impedance spectroscopy (EIS) was recorded in the same configuration at  $\eta=0.2$  V from 10<sup>-2</sup> to 10<sup>6</sup> Hz with an AC voltage amplitude of 5 mV. All the potentials were calibrated to a reversible hydrogen electrode (RHE).

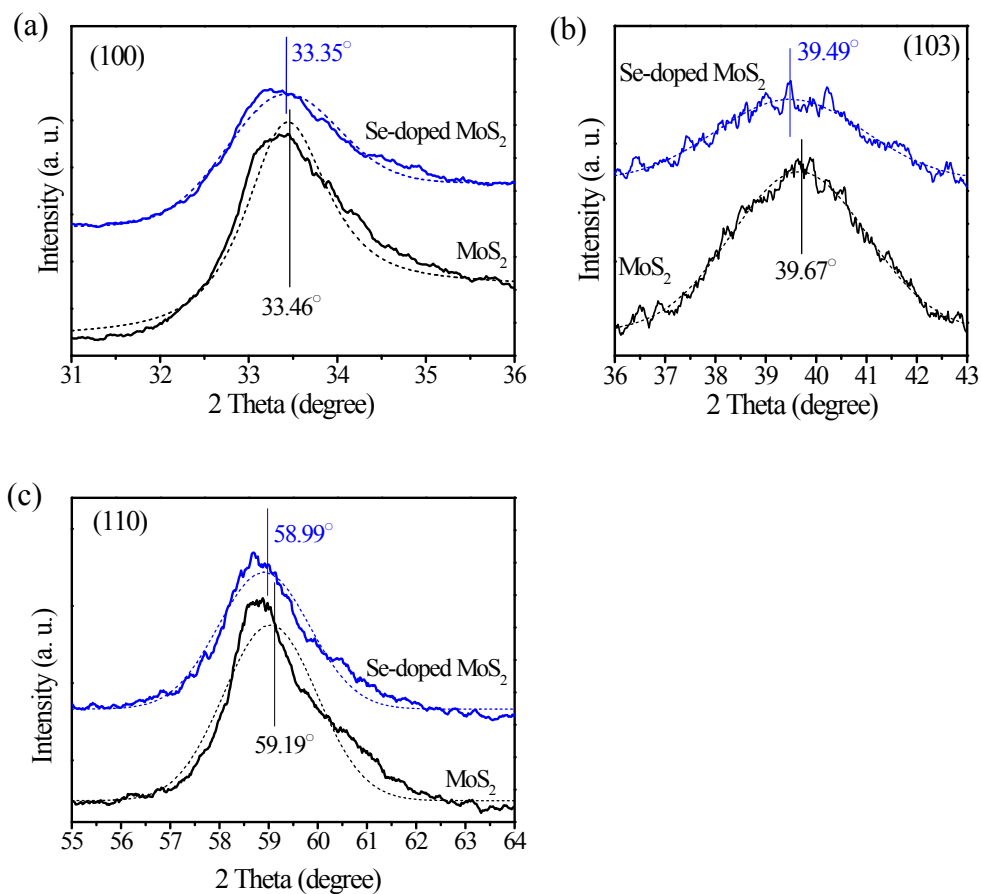


**Fig. S1** The enlarged XRD patterns showing the diffraction peak shift of (a) the (100) crystal plane, (b) the (103) crystal plane and (c) the (110) crystal plane of the MoS<sub>2</sub> and the Se-doped MoS<sub>2</sub> nanosheets. The solid lines are experimental data and the dotted lines are the corresponding Gaussian fittings.

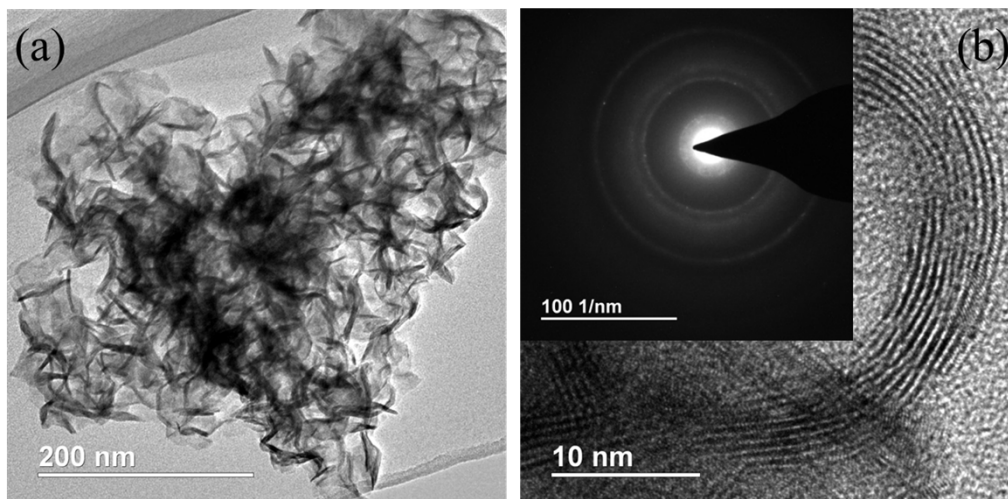


**Fig. S2** (a) TEM images of the MoS<sub>2</sub> nanosheets. (b) HRTEM image and the corresponding SAED patterns.

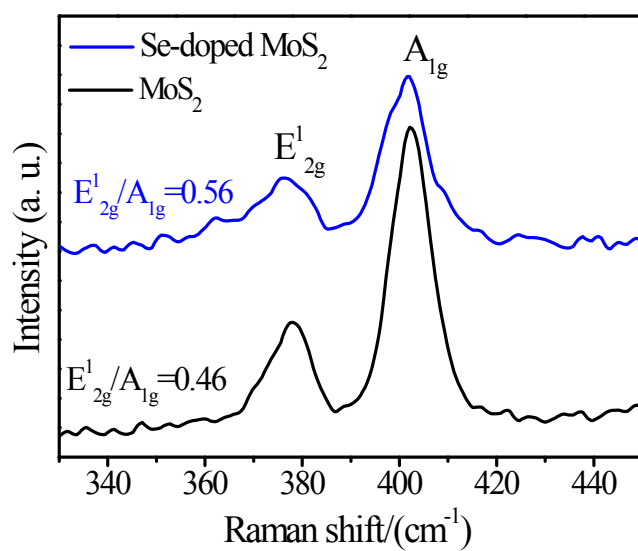


**Fig. S3** Raman spectra recorded using a 532 nm laser for the MoS<sub>2</sub> and the Se-doped MoS<sub>2</sub> nanosheets.

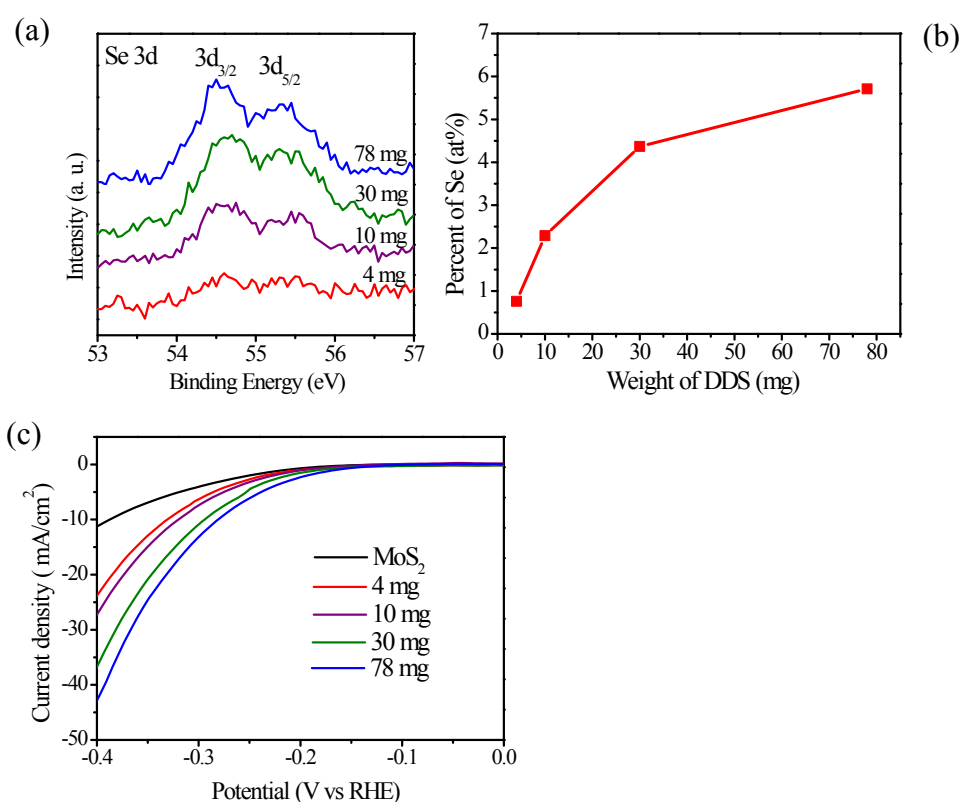


**Fig. S4** (a) Representative Se 3d XPS spectra of Se-doped MoS<sub>2</sub> samples with different weight of DDS. (b) Se doping concentration as a function of the weight of DDS. (c) Polarization curves of Se-doped MoS<sub>2</sub> vs. Se content.

Fig. S4 (a) shows Se 3d XPS spectra in the Se-doped MoS<sub>2</sub> nanosheets. It is clear that when the weight of DDS is increased from 4 mg to 78 mg, the peaks of Se 3d<sub>3/2</sub> and Se 3d<sub>5/2</sub> appear and become dominant. Fig. S4 (b) shows the atomic percentage of Se incorporated into MoS<sub>2</sub> as a function of weight of DDS. It shows that the Se percentage increased with the weight of DDS and the largest value can reach up to 5.7% with the DDS of 78 mg, indicating the enhanced doping effect of Se. The catalytic current densities of Se-doped MoS<sub>2</sub> are larger than that of pristine MoS<sub>2</sub> at a constant overpotential as shown in Fig. S4c, indicating that the Se-doped MoS<sub>2</sub> exhibits the enhanced HER catalytic activities comparing to pristine MoS<sub>2</sub>. In addition, the HER performance of the Se-doped MoS<sub>2</sub> increased with the Se content.

**Table S1.** Comparison of HER performance in acidic media for Se-doped MoS<sub>2</sub> with other state-of-the-art MoS<sub>2</sub>-based HER electrocatalysts.

Catalyst		Onset potential (mV)	Tafel slope (mV/dec)	References
Undoped MoS <sub>2</sub>	MoS <sub>2</sub> Nanosheets	-180	87	[1]
	Nanosized bulk MoS <sub>2</sub>	-280	82	[2]
	MoS <sub>2</sub> nanoparticles	-160	77	[3]
Doped MoS <sub>2</sub>	V-doped MoS <sub>2</sub>	-130	60	[4]
	Oxygen-incorporated MoS <sub>2</sub>	-120	55	[5]
MoS <sub>2</sub> /conductive substrates composites	MoS <sub>2</sub> /Graphene/Ni-foam	-109	42.8	[6]
	MoS <sub>2</sub> /RGO	-100	41	[7]
	MoS <sub>2</sub> /CNF mats	-120	45	[8]
	Se-doped MoS <sub>2</sub>	-140	55	This work

RGO: Reduction graphene oxide

CNF: Carbon fiber foam

### Quantitative XPS analysis

The doping concentration of selenium present in Se-doped MoS<sub>2</sub> nanosheets is quantified using the following equation.

$$\text{Se}/(\text{Se}+\text{S}) = (\text{I}_{\text{Se}}/\text{F}_{\text{Se}})/(\text{I}_{\text{Se}}/\text{F}_{\text{Se}}+\text{I}_{\text{S}}/\text{F}_{\text{S}})$$

where, I<sub>S</sub> and I<sub>Se</sub> are the areas under the peaks for S-2p<sub>3/2</sub> and Se-3p<sub>3/2</sub> respectively. F<sub>S</sub> and F<sub>Se</sub> are the relative symmetric factors (R.S.F) for S-2p<sub>3/2</sub> and Se-3p<sub>3/2</sub> respectively.

### References

- [1] J. Xie, H. Zhang, S. Li, R. Wang, X. Sun, M. Zhou, J. Zhou, X. W. Lou, Y. Xie, *Adv. Mater.*, 2013, **25**, 5807-5813.
- [2] T.Y. Wang, D.L. Gao, J.Q. Zhuo, Z.W. Zhu, P. Papakonstantinou, Y. Li, M. X. Li, *Chem. Eur. J.* 2013, **19**, 11939-11948.
- [3] X. Guo, G. Cao, F. Ding, X. Li, S. Zhen, Y. Xue, Y. Yan, T. Liu, K. Sun, J. *Mater. Chem. A*, 2015, **3**, 5041-5046.
- [4] X. Sun, J. Dai, Y. Guo, C. Wu, F. Hu, J. Zhao, X. Zeng and Y. Xie, *Nanoscale*, 2014, **6**, 8359-8367.
- [5] J. Xie, J. Zhang, S. Li, F. Grote, X. Zhang, H.zhang, R. Wang, Y. Lei, B. Pan, Y. Xie, *J. Am. Chem. Soc.*, 2013, **125**, 17881-17888.
- [6] Y.-H. Chang, C.-T. Lin, T.-Y. Chen, C.-L. Hsu, Y.-H. Lee, W. Zhang, K.-H. Wei, L.-J. Li, *Adv. Mater.* 2013, **25**, 756-760.
- [7] Y. Li, H. Wang, L. Xie, Y. Liang, G. Hong, H. Dai, *J. Am. Chem. Soc.* 2011, **133**, 7296-7299.
- [8] H. Zhu, M. L. Du, M. Zhang, M. L. Zou, T. T. Yang, Y. Q. Fu and J. M. Yao, *J. Mater. Chem. A*, 2014, **2**, 7680-7685.